Dynamical bistability in the driven circuit QED

V. Peano[1,3(a)] and M. Thorwart[2,3]

[1] *Physikalisches Institut, Albert-Ludwigs-Universität Freiburg - 79104 Freiburg, Germany, EU*
[2] *Freiburg Institute for Advanced Studies (FRIAS), Albert-Ludwigs-Universität Freiburg - 79104 Freiburg, Germany, EU*
[3] *Institut für Theoretische Physik, Heinrich-Heine-Universität Düsseldorf - 40225 Düsseldorf, Germany, EU*

Abstract – We show that the nonlinear response of a driven circuit quantum electrodynamics setup displays antiresonant multiphoton transitions, as recently observed in a transmon qubit device. By including photon leaking, we explain the lineshape by a perturbative and a semiclassical analysis. We derive a bistable semiclassical quasienergy surface whose lowest quasienergy eigenstate is squeezed, allowing to define a squeezing-dependent local effective temperature. We study the escape dynamics out of the metastable state and find signatures of dynamical tunneling, similar as for the quantum Duffing oscillator.

Introduction. – One of the nontrivial fundamental models of quantum physics is the Jaynes-Cummings (JC) model [1]. It was introduced to describe the interaction of a two-level atom and a single quantized electromagnetic field mode. Being sufficiently simple, its dynamics is very rich though, including Rabi oscillations, collapse and revival phenomena, squeezing, entanglement, Schrödinger cat and Fock states, and photon antibunching [2]. Beyond quantum optical set-ups, it is applicable to many situations of nanocircuit quantum electrodynamics (QED), such as Cooper pair boxes [3], superconducting flux qubits [4], Josephson junctions [5], and semiconductor quantum dots [6]. In particular, the latter setups allow to explore the regime of strong coupling and nonlinear response.

Recently, unique nonlinear features have been detected in the transmitted heterodyne signal of a superconducting transmon qubit device [7]. For weak driving, the two well-known vacuum Rabi resonances reflect transitions between the JC groundstate and the first/the second excited state of the undriven JC spectrum. Their difference in energy is $2\hbar g$, where g is the interaction strength of the qubit and the harmonic mode. For increasing driving, each vacuum Rabi peak supersplits into additional (anti-)resonances with the characteristic $\sqrt{n}$ spacing. The measurements have been corroborated with accurate numerical

simulations based on a Markovian master equation of Lindblad form [7]. For the particular case of the one-photon resonance of the JC groundstate and the antisymmetric superposition of transmon and photon excitation, an effective two-level model composed of both transmon and cavity degrees of freedom has been established. The ensuing Bloch equations have been solved analytically, yielding a closed expression for the heterodyne amplitude. For higher multiphoton resonances, the numerical solution of the master equation was compared to the experimental data, with superb agreement. However, the underlying nontrivial competition of driving and dissipation has not been discussed.

In this letter, we provide a complete physical picture for the dissipative dynamics of the Purcell-limited nonlinear response of the driven JC model in terms of quantum multiphoton (anti-)resonances. The underlying competition of driving and dissipation is revealed by perturbative arguments in the rotating frame in presence of photon leaking. We show explicitly that the lineshape of the multiphoton resonance in general is determined by the ratio of the Rabi frequency and the dissipation strength, allowing for a direct experimental control. In addition to the general analysis of the lineshapes of the multiphoton resonances, which were discussed in ref. [7] based on the numerical solution of the master equation only, we consider the semiclassical limit of the driven JC model. In the regime of strong driving, which cannot be accessed

---

(a)E-mail: vittorio.peano@physik.uni-freiburg.de

perturbatively, we derive a novel semiclassical quasi-energy surface which is *bistable*. We show that its lowest quasienergy eigenstate is an amplitude squeezed state and displays large out-of-phase oscillations. We consider the dissipative dynamics on the quasienergy surface at zero temperature. It is known that dissipation in driven nonlinear oscillators introduces nontrivial effects, such as quantum activation [8–10] and dynamic resonant tunneling [11–13]. We show that for the case of the dissipative driven JC model, the lowest quasienergy eigenstate is significantly populated at a multiphoton (anti)resonance, and is metastable away from resonance. The semiclassical analysis allows for an intuitive picture of dynamic bistability and dynamic resonant tunneling for the driven dissipative JC model, which has not been developed before. Furthermore, we reveal deep analogies with the quantum Duffing oscillator [8,10–16].

The model. – We start from a harmonic oscillator with frequency ω_r which is resonantly coupled with strength g to a qubit of the same frequency ω_r and which is driven with frequency ω_{ex} and field strength f. In the frame rotating with ω_{ex} and for $\delta\omega \equiv \omega_r - \omega_{ex}, g, f \ll \omega_r$, we perform a rotating-wave approximation and obtain the Hamiltonian of the driven JC model ($\hbar = k_B = 1$)

$$H = \delta\omega \left(a^\dagger a + \frac{\sigma_z}{2} + \frac{1}{2}\right) + \frac{g}{2}\left(a^\dagger \sigma_- + a\sigma_+\right) + \frac{f}{2}\left(a^\dagger + a\right),$$

(1)

with $\sigma_\pm = \sigma_x \pm i\sigma_y$. Here, σ_j are the Pauli matrices. The undriven JC model has the quasienergies $\varepsilon_0 = -\delta\omega/2$, $\varepsilon_{n,\pm} = (n-1/2)\delta\omega \pm g\sqrt{n}$ and the quasienergy states $|\phi_0\rangle = |0, g\rangle, |\phi_{n\pm}\rangle = (|n-1, e\rangle \pm |n, g\rangle)/\sqrt{2}$. We will refer to the latter as n-photon (dressed) states with two spin directions $\pm$. For $f \neq 0$, avoided crossings of the quasienergy levels arise, which correspond to N-photon transitions at $\delta\omega = \pm g/\sqrt{N}$. To have well-separated resonances, we consider the regime $g \gg f$. Around the resonance, the zero-photon state $|\phi_0\rangle$ and the N-photon dressed state $|\phi_{N\pm}\rangle$ display Rabi oscillations with the Rabi frequency $\Omega_N \propto f^N/g^{N-1}$.

Due to the suppression of $(1/f)$-noise, transmon qubits are Purcell-limited in the resonant regime considered here [17]. For low temperatures $T \ll \omega_{ex}$, we incorporate Purcell dissipation by means of the simple Lindblad master equation

$$\dot{\rho} = -i[H, \rho] + \frac{\kappa}{2}\left([a\rho, a^\dagger] + [a, \rho a^\dagger]\right),$$

(2)

for the reduced density operator ρ of the coupled qubit-oscillator system. Then, only photon leaking from the system into the bath is possible. Hence, in the absence of multiphoton transitions, $|\phi_0\rangle$ is dominantly populated in the stationary state. In contrast, at a multiphoton resonance, the stationary state is generated by coherent driving to the N-photon state and a subsequent relaxation via all the intermediate n-photon states ($n \leqslant N$) to the
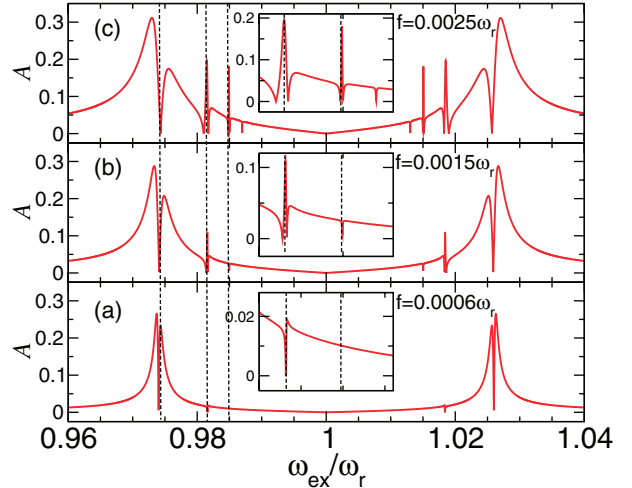

Fig. 1: (Colour on-line) Amplitude A as a function of the driving frequency ω_{ex} for $f = 0.0006\omega_r$ (a), $f = 0.0015\omega_r$ (b) and $f = 0.0025\omega_r$ (c). Insets: zooms to the corresponding (anti-)resonances marked by the dashed lines. Moreover, $g = 0.026\omega_r, \kappa = 5 \times 10^{-5}\omega_r$. A realistic value for $\omega_r/(2\pi)$ is 7 GHz [7,17].

0-photon state due to photon leaking. Eventually, this nontrivial interplay generates a stationary mixture of all n-photon states. In particular, each different choice of model parameters influences the intermediate dissipative transitions, which, in turn, determine the asymptotic populations of the stationary state.

We are interested in the nonlinear response characterized by the steady-state intracavity field $\langle a\rangle = \text{tr}(\varrho a) = Ae^{i\varphi} = \sum_{\alpha\beta}\varrho_{\alpha\beta}a_{\beta\alpha}$, where α, β refer to the quasienergy eigenstates basis. We discuss the case $\delta\omega > 0$, the opposite follows from $|\phi_{n\pm}\rangle \to |\phi_{n\mp}\rangle$, $f \to -f$ and $\varphi \to -\varphi + \pi$. The modulus A is related to the transmitted amplitude $A_{\text{tr}} \propto A$ and intensity $I_{\text{tr}} \propto A^2$ of the microwave input signal at frequency ω_{ex} [7]. In the rotating frame, $\langle a\rangle < 0$ ($\varphi = \pi$) corresponds to an oscillation out of phase with respect to the drive.

Numerical results. – The nonlinear response, in the first instance obtained from a numerical solution of eq. (2), is shown in fig. 1 for the parameters in the regime of ref. [7]. The drive induces a splitting of the vacuum Rabi resonance and produces two families of peaks which are symmetric with respect to $\omega_{ex} = \omega_r$ and which are associated to the $\pm$ quasienergy states. In each family, (anti)resonances occur which correspond to multiphoton transitions and which are associated to the avoided crossings of quasi-energy levels, see fig. 2(c). We note that no antiresonances occur in the photon number $\langle a^\dagger a\rangle$ [18].

For weak driving (fig. 1(a)), only the 1-photon antiresonance is well pronounced. It can be described [7,13] by a model involving the 0- and the 1-photon state. The generic mechanism is that, at resonance, they are equally populated and oscillate with opposite phase yielding zero response. Slightly away from resonance, one of the two
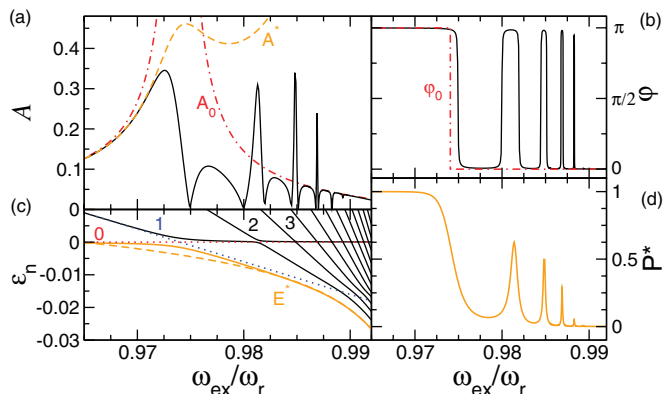
Fig. 2: (Colour on-line) Nonlinear response of the driven JC model: (a) amplitude, (b) phase, (c) quasienergies, and (d) population of the lowest quasienergy state $|\psi^*\rangle$ for $g = 0.026\omega_\mathrm{r}, f = 0.004\omega_\mathrm{r}, \kappa = 10^{-4}\omega_\mathrm{r}$. Dash-dotted red line in (a),(b): lowest-order result for non-resonant approximation. Dashed orange line in (a): $A^* = |\langle\psi^*|a|\psi^*\rangle|$; and in (c): semi-classical result eq. (6) for the lowest quasienergy E^*.

states is more populated and a finite response arises. Far away from the resonance, the response again approaches zero. Overall, the lineshape of an antiresonance arises. The antiresonance around $\omega_\mathrm{ex} \approx 0.98\omega_\mathrm{r}$ corresponds to a 2-photon process (fig. 1(a)). This feature also follows from a two state description. The shape is different from the 1-photon antiresonance, due to the background contribution of nonresonant 1-photon mixing processes [16].

For increasing driving, unexpected features arise. The multiphoton antiresonances turn into resonances, see figs. 1(b) and (c). Associated to the behavior of A are jumps in the phase φ, see fig. 2(b). This already suggests that two quasienergy states —one oscillating in and one out of phase— are alternately populated. Interestingly, the population (fig. 2(d)) of the state $|\psi^*\rangle$ with lowest quasienergy shows peaks at the resonance frequencies. In fact, as we will show below, $|\psi^*\rangle$ is localized in the bottom of a well of a bistable quasienergy surface. $|\psi^*\rangle$ is metastable since the bath induces transitions to higher quasienergies states and an escape is always possible, even at zero temperature. This feature has also been reported for the quantum Duffing oscillator [11–13].

Perturbative approach. – These observations are further substantiated by perturbative arguments, which show how the asymptotic populations of the stationary state are determined by the various rates of the intermediate dissipative transition processes. Here, we assume that the dressed states $|\phi_{n\pm}\rangle$ ($n \neq N$) are approximate eigenstates. In the next section we will show that this is true only for very weak driving fields.

Out of resonance, $\rho_{00} \simeq 1$ yielding $\langle a\rangle \simeq -f[(\delta\omega + g)^{-1} + (\delta\omega - g)^{-1}]/4$ up to first order in f. As follows from figs. 2(a) and (b) (dash-dotted red lines), the lowest-order response A_0 coincides with the exact one away from

resonance. Moreover, $\varphi_0 = \pi$ for $\delta\omega \leqslant g$ and $\varphi_0 = 0$ for $\delta\omega > g$.

At the N-photon-resonance, the system can leave $|\phi_0\rangle$ by tunneling to $|\phi_{N-}\rangle$ and the bath induces decays from $|\phi_{n-}\rangle$ to $|\phi_{n-1-}\rangle$ along the ladder $N \to N-1 \to \ldots \to 1 \to 0$. The decay rates (in secular approximation) are readily evaluated from eq. (2) as $\mathcal{L}_{n-,(n-1)-} = (\sqrt{n} + \sqrt{n-1})^2\kappa/4$ for $n \neq 1$ and $\mathcal{L}_{1-,0} = \kappa/2$. Hence, the rate from the 1-photon to the 0-photon state is smallest. Note that the probability of a decay to a state with opposite dressed spin is small, i.e., $\mathcal{L}_{(n-1)-,n+}/\mathcal{L}_{(n-1)+,n+} \simeq 1/[16n(n-1/2)]$. Hence, the population of the 1-photon state is always larger than those of the n-photon states. In addition, depending on the ratio κ/Ω_N, qualitatively different stationary populations arise from a competition between tunneling from $|\phi_0\rangle$ to the top of the ladder, $|\phi_{N-}\rangle$, and relaxation down the ladder. For $\kappa \gg \Omega_N$, the population of $|\phi_0\rangle$ is $\simeq 1$, because damping is more efficient than tunneling. Dissipation then completely washes out the resonance, and the response is the same as that off resonance and thus is in phase with the drive. For $\kappa \simeq \Omega_N$, a small population ρ_{11} emerges, contributing $\rho_{11}a_{11}$ with $a_{11} = \frac{f}{2(\varepsilon_{1-}-\varepsilon_{2-})}\frac{3+2\sqrt{2}}{4} + \frac{f}{4(\varepsilon_{1-}-\varepsilon_0)} < 0$ since, in the perturbative regime and for $N < 6$, $\varepsilon_{1-} < \varepsilon_{2-}, \varepsilon_0$. This leads to a reduced response, forming an antiresonance, see, e.g., the 2-photon antiresonance shown in fig. 1(a). For $\kappa \ll \Omega_N$, tunneling is faster than relaxation and the population of $|\phi_{1-}\rangle$ becomes the largest. Then, the contribution $\rho_{11}a_{11} < 0$ dominates, leading to an out-of-phase oscillation. To be specific, for the 2-photon resonance of fig. 1, $\kappa/\Omega_2 = \kappa g(\sqrt{2}f^2) = 1.8$ (a), 0.29 (b) and 0.1 (c).

Semiclassical approach. – For increasing (but still weak) driving, the response is qualitatively similar, although the perturbative approach becomes inadequate. In fact, as shown in fig. 2(d), at resonance, there is a large population P^* of the lowest quasienergy state $|\psi^*\rangle$. As follows from fig. 2(c), $|\psi^*\rangle \neq |\phi_{1-}\rangle$. In order to account for the importance of $|\psi^*\rangle$, we perform next a semiclassical analysis. We switch to the dressed atom picture, by means of the unitary transformation

$$R = \exp\left(\frac{-3\pi}{8\sqrt{a^\dagger a + \sigma_z/2 + 1/2}}[a^\dagger\sigma_- - a\sigma_+]\right), \quad (3)$$

mapping the JC eigenstates into product states $|n\sigma\rangle$ (with $\sigma = g, e$). Under this transformation, the undriven JC Hamiltonian becomes diagonal in the spin degrees of freedom and reads

$$\tilde{H} = |\delta\omega|\left(a^\dagger a + \frac{\sigma_z}{2} + \frac{1}{2}\right) + g\sigma_z\sqrt{a^\dagger a + \frac{\sigma_z}{2} + \frac{1}{2}}, \quad (4)$$

while $\tilde{a} = R^\dagger a R = a + \mathcal{O}(n^{-1/2})$. This expression follows by expanding the matrix elements of the creation operator in the dressed Fock basis with respect to n. Higher-order terms include spin flipping operators. Next, we

introduce the canonical variables $\mathcal{X} = \sqrt{\lambda/2}(a^\dagger + a)$ and $\mathcal{P} = i\sqrt{\lambda/2}(a^\dagger - a)$, where $\lambda = \delta\omega^2/g^2$ is a dimensionless parameter playing the role of $\hbar$. Eventually, neglecting all higher-order terms, we obtain the transformed Hamiltonian $\tilde{H} \simeq \delta\omega\lambda^{-1}Q(\mathcal{X},\mathcal{P})$ with

$$Q(\mathcal{X},\mathcal{P}) = \frac{\mathcal{X}^2}{2} + \frac{\mathcal{P}^2}{2} + \sigma_z\sqrt{\frac{\mathcal{X}^2}{2} + \frac{\mathcal{P}^2}{2}} + \frac{f}{\sqrt{2}g}\mathcal{X}. \quad (5)$$

It can be interpreted as a quasienergy surface in phase space and is visualised in fig. 3. For $\sigma_z = -1$ (fig. 3(a), an internal dome appears around $\mathcal{X} = 0, \mathcal{P} = 0$, such that two quasiclassical orbits encircle the inner maximum, one on the external and one on the internal domain. They are degenerate with respect to their quasienergies and thereby define a dynamical bistability. Both domains are separated by the separatrix shown in fig. 3(a) as the oriented black solid line. The overall shape of the quasienergy surface resembles a Mexican hat. The drive induces a finite tilt of the surface, generating a quasienergy well around the quasienergy minimum. The orbits near the inner maximum correspond to small photon numbers and are not accurately described by the semiclassical approach. On the other hand, the orbits on the outer domain correspond to states with large photon numbers. Deep in the quantum regime, discrete multiphoton transitions correspond to tunneling transitions between these quasiclassical orbits. The surface for the opposite dressed spin orientation $\sigma_z = +1$ is a less interesting monotonous function, shown in fig. 3(b).

Let us next consider the dynamics around the minimum located at $\mathcal{P}_{\min} = 0$ and $\mathcal{X}_{\min} = -(f/g + 1)/\sqrt{2}$. A harmonic expansion yields the quasienergy E^* for the state localized at the bottom of the quasienergy surface as $E^* = \delta\omega\lambda^{-1}[Q(\mathcal{X}_{\min}, 0) + (\lambda/2)\omega^*]$, or written in terms of f and g as

$$E^* = -\frac{g^2}{4\delta\omega}\left(\frac{f}{g} + 1\right)^2 + \frac{\delta\omega}{2}\sqrt{\frac{f}{g+f}}, \quad (6)$$

with the effective frequency $\omega^* = \sqrt{f/(g+f)}$. This result is correct up to $\mathcal{O}(\lambda^2)$ and is shown in fig. 2(c) as orange dashed line. It almost coincides with the exact result, even for small photon numbers $N = 1$.

Up to leading order in λ, the lowest quasienergy eigenstate

$$|\psi^*\rangle = R^{-1}D(\mathcal{X}_{\min})S(r)|0\,g\rangle \quad (7)$$

is obtained by applying to the vacuum: i) the squeezing operator $S(r) = \exp[r(a^2 - a^{\dagger 2})/2]$ with squeeze factor $r = -(\ln\omega^*)/2 = \ln[1 + g/f]/4$, ii) the translation $D(\mathcal{X}_{\min}) = \exp[i\mathcal{P}\mathcal{X}_{\min}/\lambda]$ to the minimum, and iii) R^{-1} to return to the bare atom picture. With this, one can compute the Fock-state representation [19] and all expectation values at leading order. It turns out that $|\psi^*\rangle$ has sub-Poissonian statistics and shows photon antibunching. This is not surprising, in fact $D(\mathcal{X}_{\min})S(r)|0\,g\rangle$ is an amplitude squeezed state for $r > 0$.
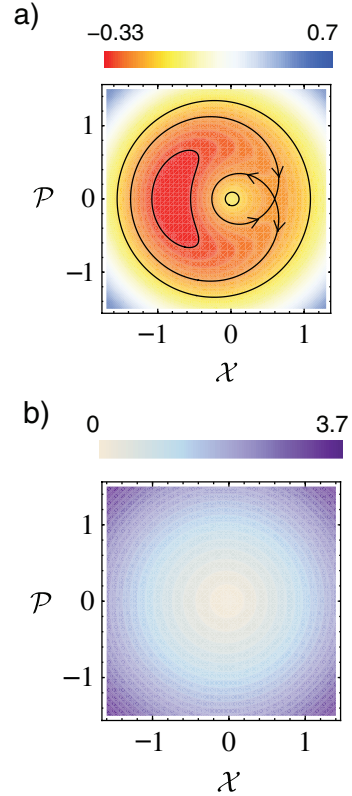
Fig. 3: (Colour on-line) Contour plot of the quasienergy surfaces $Q(\mathcal{X},\mathcal{P})$ for the dressed spin orientation $g\,(\sigma_z = -1)$ (a) and $e\,(\sigma_z = +1)$ (b) for $f = 0.004\omega_r$ and $g = 0.026\omega_r$, yielding $f/g = 0.154$ and $T_{\text{eff}} = 0.65$. The solid black lines in (a) indicate quasiclassical orbits and include also the separatrix between the two domains of attraction.

Note that this state $|\psi^*\rangle$ exists for any finite driving strength (provided that λ be much smaller than the barrier height f/g), but it is not present in the undriven case. For this reason it is not possible to describe it in terms of simple perturbation theory in the driving. In fact, in the limit of vanishing driving, the tilt of the quasienergy surface vanishes and no quasienergy well is developed. For weak but finite driving, the well is still very shallow in the momentum direction, allowing for large momentum fluctuations of a state confined in it. For increasing driving, the well becomes deeper and more symmetric. For this reason, the squeezing factor decreases for increasing driving. Let us furthermore emphasize that $|\psi^*\rangle$, *i.e.*, the lowest quasienergy eigenstate of the driven JC Hamiltonian, cannot be identified with the squeezed state investigated in ref. [20] (for $\delta\omega = 0$).

The latter is the eigenstate obtained by starting in the JC groundstate $|\phi_0\rangle$ and by switching on adiabatically the driving. It has vanishing quasienergy for $\delta\omega \to 0$. Moreover, it tends to follow the driving by rotating its spin part and squeezing its amplitude fluctuations. Hence, as opposed to $|\psi^*\rangle$, its squeezing factor *increases* for increasing driving. We expect the Wigner representation for this state to be confined in an area of size λ^2 around

the local quasienergy maximum. Unfortunately, it cannot be incorporated in our semiclassical description because it corresponds to a small photon number. In the following discussion, we will assume that $f \ll g$, so that perturbation theory is still valid close to *zero* quasienergy (although it is not valid close to the quasienergy minimum). In this case, the JC groundstate $|\phi_0\rangle$ is still an approximate eigenstate of the driven JC Hamiltonian.

Next, we consider the dissipative semiclassical dynamics. As will be shown below, a separation of time scales exists which defines a fast intrawell and a slow interwell relaxation. Deep in the semiclassical limit, the quasienergy states, localized close to the minimum of one well, can be obtained as $|\psi_n^*\rangle = R^{-1}b^{\dagger n}R|\psi^*\rangle/\sqrt{n!}$ with $b = a\cosh r + a^\dagger \sinh r - e^r \mathcal{X}_{\min}/\sqrt{2\lambda}$. In this limit, dissipative transitions occur only between nearest neighbors, with the rates $\mathcal{L}_{n-1,n} = \kappa n \cosh^2 r$, $\mathcal{L}_{n,n-1} = \kappa n \sinh^2 r$. Here, the detailed balance condition is fullfilled. When the system is initially in a state with a large photon number, it has a large probability to fall in the basin of attraction of the quasipotential minimum (intrawell relaxation). When also $\kappa \ll g\lambda\omega^*$, detailed balance determines an effective Boltzmann distribution $P_n^* = P^* e^{-n\beta_{\rm eff}}$, with effective inverse temperature $\beta_{\rm eff} = 2\ln\coth r$. We emphasize that this link between effective temperature and squeezing can be generalized to any driven quantum system with a smooth quasienergy surface and coupled linearly to a bath (*e.g.*, the Duffing oscillator [8,10–16] or the parametrically driven oscillator [9]). It can be easily generalized to finite temperatures $T > 0$ as well. It turns out that the zero-temperature limit applies when $\sinh^2 r$ is much larger than the bosonic occupation number $\bar{n}(\omega_{\rm ex}/T)$ of the bath at $\omega_{\rm ex}$. In the opposite limit, $\beta_{\rm eff} = \omega_{\rm ex}/T$. Since we include here only photon leaking, *i.e.*, $\omega_{\rm ex} \gg T$, the effective temperature is still small.

On the large time scale, the system decays to the 0-photon state with a forward rate k_+ for the interwell relaxation. From there, it can return to the basin of attraction of the minimum by a driving induced transition with a backward rate k_-. The stationary populations of the intrawell states (oscillating out of phase) and the 0-photon state (in phase) are determined by the ratio k_+/k_-. Off resonance, photon leaking favors the 0-photon state and $k_+ \gg k_-$. Approaching a resonance, k_- increases due to an increasing contribution due to tunneling to the escape. When the tunneling contribution becomes comparable to k_+, the response is qualitatively modified yielding an (anti-)resonance.

To render the qualitative discussion more quantitative, we consider the eigenvalues of the Liouville operator which governs the Lindblad master equation (2). We start deep in the semiclassical regime, *i.e.*, for small detuning, where $\omega_{\rm ex} \approx \omega_{\rm r}$. Here, a clear separation of time scales for the dissipative dynamics on the bistable quasienergy surface occurs. Well-defined energy wells with a large quasienergy barrier in between exist for small detuning and allow for a clear description in terms of a single relaxation rate (see
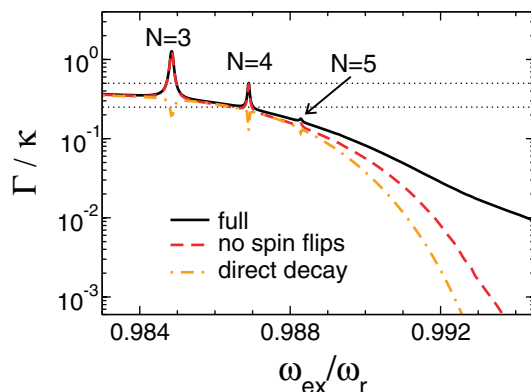

Fig. 4: (Colour on-line) Solid line: Smallest eigenvalue of the Lindblad master equation. Dashed red line: the same without dissipative spin flips. Dash-dotted orange line: decay rate for $|\psi^*\rangle \to |\phi_0^f\rangle$. Dotted lines correspond to $\kappa/2$ and $\kappa/4$. The parameters are $g = 0.026\omega_{\rm r}$, $f = 0.004\omega_{\rm r}$, and $\kappa = 10^{-4}\omega_{\rm r}$.

also ref. [21]). In this regime, we find a single eigenvalue Γ which consists of the sum of k_- and k_+, is real and much smaller than the real parts of all the other eigenvalues. This is shown in fig. 4 as black solid line. For increasing detuning, *i.e.*, when $\omega_{\rm ex} \lesssim 0.987\omega_{\rm r}$ in fig. 4, we enter a regime, where the separation of time scales is not so clearly expressed and Γ becomes comparable to the real parts of three more eigenvalues. The latter correspond to relaxation (one real eigenvalue) and to decoherence (a complex-conjugated pair of eigenvalues) involving the pair of states $|\phi_{1+}\rangle$ and $|\phi_0\rangle$. We do not show them in the figure, but instead show the perturbatively determined values $\kappa/2$ (relaxation) and $\kappa/4$ (decoherence) out of resonance as dotted horizontal lines. The peaks in fig. 4 (black solid lines) are due to tunneling from the 0- to N-photon state. When the Rabi frequency Ω_N is much larger than the N-photon dressed-state decay rate Γ_N, the system tunnels back and forth many times between the two internal domains of the quasienergy surface, before it decays to the external domain with rate $k_- \approx \Gamma_N/2$. In the opposite limit $\Gamma_N \gg \Omega_N$, the tunneling rate is reduced due to the quasienergy level fluctuations. It becomes equal to Ω_N^2/Γ_N [22] and coincides approximately with the escape rate k_-. Away from resonance, $\Gamma \approx k_+$.

There are three mechanisms of decay from the metastable well: i) The system can decay directly to the 0-photon state with the rate shown in fig. 4, dash-dotted orange line. ii) The system can climb up the quasienergy well by quantum activation [8]. Both associated rates are expected to decrease exponentially, following $\propto e^{-c_i/\delta\omega^2}$, with some constants c_i (the prefactor varies smoothly with $\delta\omega$), which defines the separation of time scales. iii) For very small detuning, the escape occurs via bath-induced spin flips. In fact, this mechanism is suppressed only as a power-law $\Gamma \propto \delta\omega^2$. To separate ii) from iii), we show Γ without the bath-induced spin flips in fig. 4 (dashed red line), illustrating that spin flips are dominant when the separation of time scales is well defined. Since only a few

states close to the bottom are populated, our solution is stable against a small dephasing of the oscillator [9] or an intrinsic spin relaxation that violates detailed balance. The induced spin-flip rate would be small and remain finite for $\lambda \to 0$, imposing an upper limit to the lifetime of $|\psi^*\rangle$.

Perspectives and conclusions. – The transformation of the driven JC Hamiltonian to the quasienergy picture defined by eq. (5) allows for a quantitative semiclassical WKB analysis in the spirit of refs. [8,9]. We defer this to a future publication since it lies beyond the scope of this letter. Our analysis can be easily extended to any driven nonlinear oscillator coupled bilinearly to a thermal bath. For example, the Duffing oscillator is characterized by two classical stable solutions with different amplitudes and opposite oscillation phase. The two states can be associated with classical orbits in a quasienergy landscape which also assumes the form of a tilted Mexican hat [15] like for the JC model. Transitions between the two states can be induced by three mechanisms: i) thermal activation "over the barrier" [14,15], where the thermal fluctuations provide the energy for classical escape, ii) quantum activation [8] where bath zero-point quantum fluctuations induce a diffusive motion on the quasienergy surface over the barrier, which even at zero temperature can lead to escape, and iii) quantum tunneling [11–13].

For weak driving, the small-oscillation solution can be identified with the 0-photon quantum state. Since it is favored by photon leaking, it has a low effective temperature and can be regarded as stable in the absence of tunneling. However, this stable state is associated to a relative quasienergy maximum, in contrast to the case of a static bistable potential. At a multiphoton resonance, this state becomes metastable and generates an (anti-)resonance of the stationary oscillation and tunneling peaks in the interwell relaxation rate as a function of the detuning. These features has been already predicted in refs. [11–13], but the link to the semiclassical picture was not drawn.

Note that our results on the resonant tunneling transitions in interwell dissipative dynamics is not in contradiction with the findings of ref. [8]. There, it has been shown that the quantum activation rate is always larger than that of dissipative tunneling when they are computed semiclassically with logaritmic precision. Here and in refs. [11–13], we show that tunneling is the dominating escape mechanism in the complementary *deep quantum regime* when it is coherent and/or only very few states are confined within the quasienergy well (so that logaritmic corrections are relevant).

We furthermore note that the dissipative quantum Duffing oscillator could be realized in a Josephson bifurcation amplifier [23] operating in the quantum regime.

In conclusion, inspired by recent experiments, we have explained the nonlinear response of the driven dissipative Jaynes-Cummings model. We have predicted the existence of a metastable squeezed state in the semiclassical limit and drawn a link between effective local temperature and the squeezing parameter. We have analyzed the escape mechanisms from the metastable states and found resonant dynamical tunneling. Our analysis reveals generic features on the dissipative dynamics of nonlinear driven quantum systems for the example of the driven Jaynes-Cummings model, realized in terms of a nanocircuit QED setup.

$$* * *$$

REFERENCES

[1] Jaynes E. T. and Cummings F. W., *Proc. IEEE*, **51** (1963) 89.
[2] Larson J., *Phys. Scr.*, **76** (2007) 146.
[3] Wallraff A. *et al.*, *Nature*, **431** (2004) 162.
[4] Chiorescu I. *et al.*, *Nature*, **431** (2004) 159.
[5] Hatakenaka N. and Kurihara S., *Phys. Rev. A*, **54** (1996) 1729.
[6] Winger M., *Phys. Rev. Lett.*, **101** (2008) 226808.
[7] Bishop L. S. *et al.*, *Nat. Phys.*, **5** (2009) 105.
[8] Dykman M. I. and Smelyanskii V. N., *Sov. Phys. JETP*, **67** (1988) 1769.
[9] Marthaler M. and Dykman M. I., *Phys. Rev. A*, **73** (2006) 042108.
[10] Dykman M. I., *Phys. Rev. E*, **75** (2007) 011101.
[11] Peano V. and Thorwart M., *Phys. Rev. B*, **70** (2004) 235401.
[12] Peano V. and Thorwart M., *Chem. Phys.*, **322** (2006) 135.
[13] Peano V. and Thorwart M., *New J. Phys.*, **8** (2006) 21.
[14] Dykman M. I. and Krivoglaz M. A., *Physica A*, **104** (1980) 480.
[15] Dmitriev A. P. and D'yakonov M. I., *Sov. Phys. JETP*, **63** (1986) 838.
[16] Dykman M. I. and Fistul M. V., *Phys. Rev. B*, **71** (2005) 140508(R).
[17] Houck A. A. *et al.*, *Phys. Rev. Lett.*, **101** (2008) 080502.
[18] Chough Y. T., Nha H. and An K., *J. Phys. Soc. Jpn.*, **69** (2000) 4060.
[19] Yuen H. P., *Phys. Rev. A*, **13** (1976) 2226.
[20] Milburn G. and Alsing P., in *Directions in Quantum Optics*, edited by Carmichael H. J., Glauber R. J. and Scully M. O., *Lect. Notes Phys.*, Vol. **561** (Springer, Berlin) 2001, pp. 303–312.
[21] Hänggi P., Talkner P. and Borkovec M., *Rev. Mod. Phys.*, **62** (1990) 251.
[22] Dykman M. I. and Tarasov G. G., *Sov. Phys. JETP*, **47** (1978) 557.
[23] Siddiqi I. *et al.*, *Phys. Rev. Lett.*, **93** (2004) 207002.